Available online at www.sciencedirect.com
SCIENCE DIRECT
Polymer 47 (2006) 1172–1178
polymer
www.elsevier.com/locate/polymer

Influence of the solvent and the end groups on the morphology of cross-linked amphiphilic poly(1,2-butadiene)-*b*-poly(ethylene oxide) nanoparticles

Michael Maskos [1]

Department of Chemistry, McGill University, 801 Sherbrooke W., Montreal, Que., Canada H3A 2K6

Received 1 June 2005; received in revised form 6 December 2005; accepted 9 December 2005
Available online 9 January 2006

Abstract

The phase diagrams of nanoparticles based on self-assembled amphiphilic poly(1,2-butadiene)-*b*-poly(ethylene oxide) diblock copolymers (PB-*b*-PEO) and subsequent intra-micellar cross-linking in methanol and water show that the obtained morphology of the nanoparticles depends on: (i) the block ratio; (ii) the block length; (iii) the solvent; and (iv) the PEO-sided end group. Depending on these parameters, spherical, cylindrical and vesicle-like nanoparticles are synthesized. The PEO-sided end group is found to have an influence on the morphology of the nanoparticles and in addition, it has an impact on the characteristic dimension of the polymeric nanoparticles.

Keywords: Diblock copolymers; Self assembly; Nanoparticles

1. Introduction

The self-assembly of amphiphilic diblock copolymers in selective solvents is a steadily growing research field due to potential applications for e.g. the synthesis of novel drug delivery and targeting systems or carrier systems for diagnostic applications. Many examples can be found in the literature and these have led to an increased understanding of the development of the different morphologies built in solution [1–20]. Due to the non-covalent nature of the structure formation of these micellar aggregates, they disassemble upon addition or exchange of the selective to a less selective or a good solvent for both blocks. Intra-micellar cross-linking avoids this disintegration by the formation of covalent bonds. Examples based on diblock copolymers are reported by several authors [21–34]. Many of these systems need a co-solvent for the induction of the self-assembly process, because the glass transition temperature T_g of the core-forming block is too high [21–24]. Others need the addition of a cross-linking agent [26–34]. In order to avoid additional solvent or cross-linker, which might be difficult for potential biological applications, a low T_g-core-forming block and the direct dissolution of the diblock copolymer in the selective solvent is employed together with the cross-linking of the micellar structures by γ-irradiation. The obtained nanostructures are stable upon transfer into good solvents. In addition, it has been possible to show that the phase diagram of the diblock copolymers in water as reported by Bates et al. could be projected to the cross-linked nanoparticles.

2. Experimental

All reactions were performed under dry argon. THF p.a. (Riedel de-Haen) was dried over $LiAlH_4$ (Fluka) and degassed by three freeze–thaw cycles under high vacuum. Methanol p.a. (Merck) was distilled from azobisisobutyronitrile (AIBN, Aldrich). Ethylene oxide (Fluka) was purified over calcium hydride (Aldrich). α-Methylstyrene was distilled in vacuo. The 1,3-butadiene as well as succinic anhydride, perchloric acid (70%), acetic acid, 1,4-bis(5-phenyloxazol-2-yl)benzol (POPOP), silver acetylacetonate, sodium and potassium (Aldrich) were used as received in p.a. grade.

The ^1H NMR spectra were recorded on a Bruker AM-400, the chemical shifts are obtained by comparison with the solvent $CDCl_3$. The MALDI-TOF (matrix assisted laser desorption ionization time-of-flight) mass spectra were recorded with a Micromass Tof-Spec E in linear mode. Solutions of the matrix

E-mail address: maskos@uni-maniz.de
[1] Present address: Institut für Physikalische Chemie, Universität Mainz, Welder Weg 11, D-55099 Mainz, Germany.

0032-3861/$ - see front matter © 2005 Elsevier Ltd. All rights reserved.
doi:10.1016/j.polymer.2005.12.045

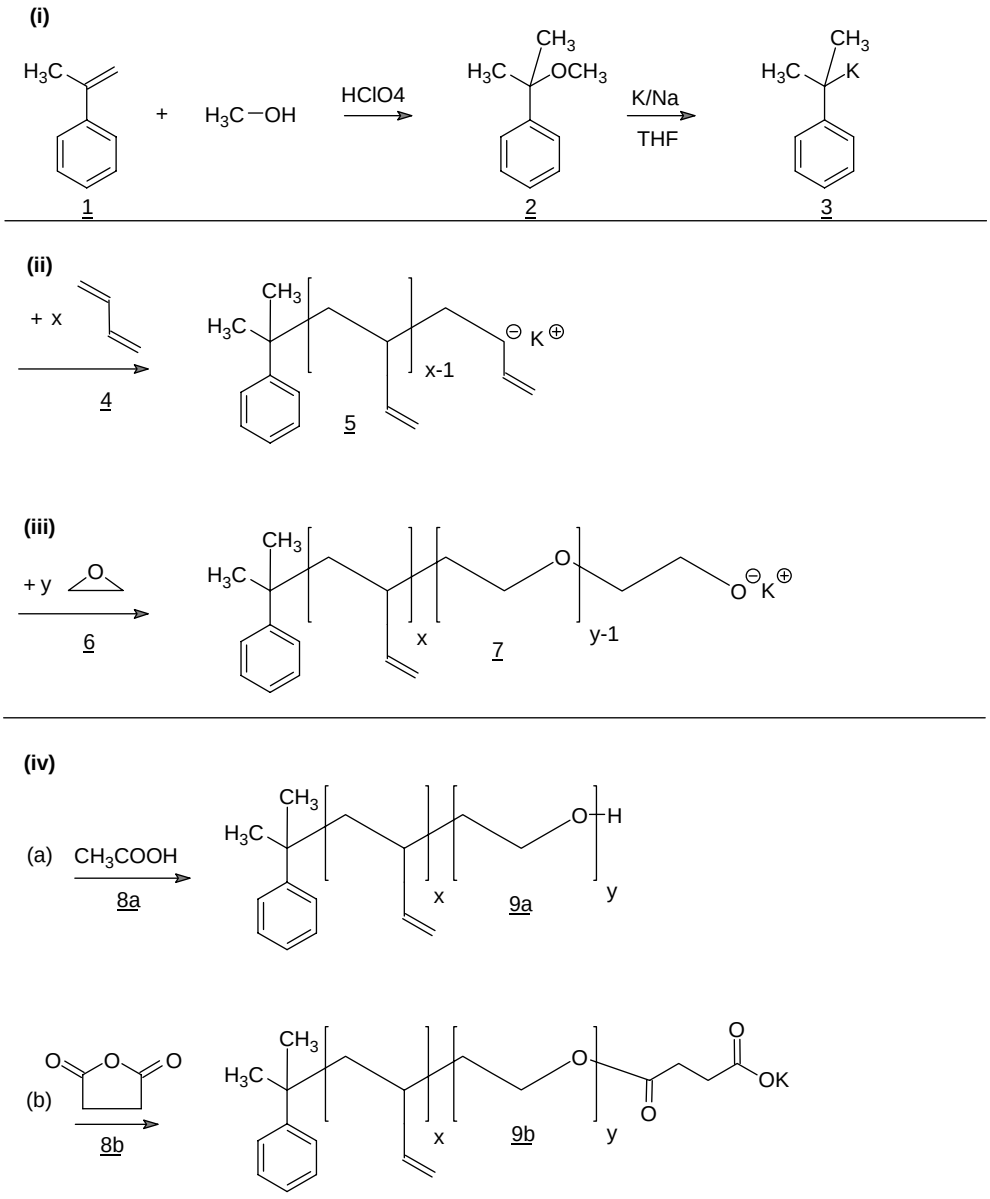

Fig. 1. Reaction scheme for the synthesis of the amphiphilic PB-*b*-PEO diblock copolymers.

[1,4-bis(5-phenyloxazol-2-yl)benzene (POPOP)] (10 g/L), silver acetylacetonate (10 g/L) and the polymer (1 g/L), all in THF, were mixed 5:2:5 v/v and 1 μL of this solution was deposited on a steel target and after drying, were injected.

GPC traces were obtained with three styragel columns (nominal pore sizes 100, 500, 1000 Å), a Waters-510 pump, a Rheodyne 7125 injection valve with a 20 μL sample loop, and a Waters-410-refractive-index (RI) detector using degassed THF as the eluent.

Cross-linking in solution was performed in glass vials at the MDS Nordion Facility, Laval, Que., Canada with ^{60}Co γ-irradiation, operated at 8.87 kGy/h. A total dose of 200 kGy has been applied to all samples to ensure complete cross-linking (exception: determination of the degree of conversion, see below).

TEM measurements were performed with a Zeiss EM900 microscope, operated at 80 kV, on carbon coated Cu-grids,

Table 1
Characterization of the PB-*b*-PEO diblock copolymers

Polymer	MALDI-TOF MS		% PEO (w/w)
	M_n (g/mol)	M_w/M_n	
$PB_{32}PEO_{29}$–H	3130	1.03	43
$PB_{32}PEO_{29}$–COOK	3315	1.03	43
$PB_{32}PEO_{52}$–H	4150	1.04	57
$PB_{32}PEO_{52}$–COOK	4320	1.04	57
$PB_{130}PEO_{66}$–H	10,800	1.05	29
$PB_{130}PEO_{66}$–COOK	11,000	1.05	29
$PB_{130}PEO_{120}$–H	13,100	1.05	43
$PB_{130}PEO_{120}$–COOK	13,200	1.06	43
$PB_{130}PEO_{177}$–H	14,400	1.06	53
$PB_{130}PEO_{177}$–COOK	14,700	1.06	53

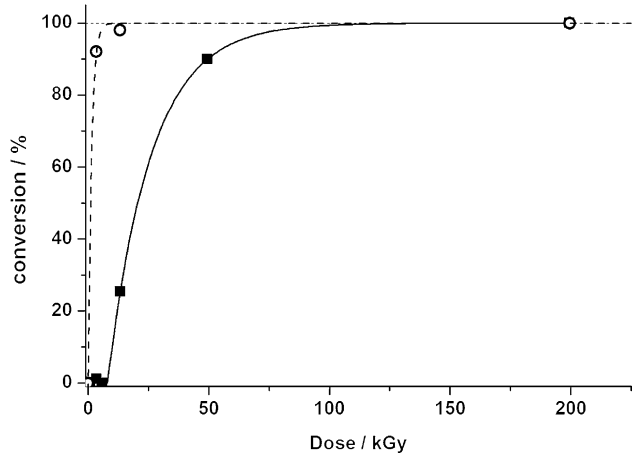

Fig. 2. Conversion of the cross-linking reaction as determined by GPC for PB_{130}–PEO_{120}–H; open circles: water, closed squares: methanol; $c = 1.0$ g/L; fit, exponential growth.

negatively stained with uranyl acetate and with a JEOL JEM-2000 FX, operated at 80 kV, on carbon coated Cu-grids. Cryo-TEM was performed with a Philips Tecnai F30, operated at 300 kV, on holy carbon coated cupper grids.

A schematic representation of the synthetic route for the synthesis of the diblock copolymers is given in Fig. 1.

The initiator cumyl potassium **3** was synthesized by acid-catalyzed addition of methanol to α-methylstyrene **1** and reaction with sodium/potassium alloy as described in the literature [35].

The anionic polymerization of 1,3-butadiene was performed at −65 °C in THF, which yields primarily 1,2-addition [35,36]. As an example, the polymerization was performed as follows: to 250 mL THF containing cumyl potassium ($c = 0.084$ mol/L) 39.5 g (0.732 mol) 1,3-butadiene **4** was added and after 1 h, a small amount of ethylene oxide **6** (4.50 g, 0.101 mol) was added to the reaction mixture, which was stirred overnight at room temperature. From the solution containing the living polymer, two aliquots were taken (I, 28.0 g, 10.5 wt% of the reaction mixture; II, 53.0 g, 19.9 wt%) and further ethylene oxide was added to each (I, 5.3 g, 0.120 mol; II, 6.2 g 0.141 mol). After 48 h at room temperature, each solution was again divided into halves and one half was terminated with 20 mL of a solution containing 2 mL of acetic acid in 100 mL THF (X = –H); the other, with 20 mL of a solution of 6 g (60 mmol) succinic anhydride in 100 mL THF (X = –(CO)–CH_2–CH_2–COOK, abbreviated –COOK). All solutions were stirred over night. The solvent was evaporated and the polymer was lyophilized from benzene. The polymer yield was in all samples larger than 85%.

The result of the characterization of the synthesized polymers is presented in Table 1. The GPC traces showed

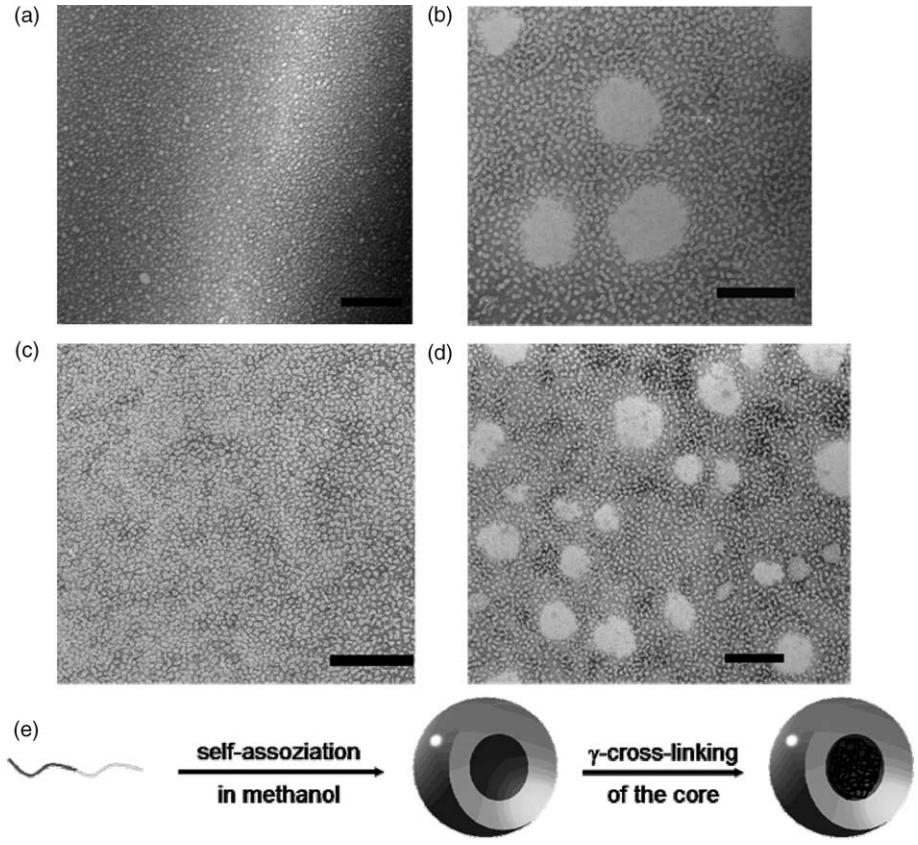

Fig. 3. TEM pictures of PB_{32}–PEO_{29}–H (a) and (b) and PB_{32}–PEO_{29}–COOK (c) and (d), after cross-linking in methanol ((a) and (c) $c = 0.5$ g/L) and after transfer of the fixed nanoparticles into THF ((b) and (d) $c = 0.5$ g/L); negatively stained with uranyl acetate ((a) and (c) 2 wt% aqueous solution, (b) and (d) saturated solution in DMF, larger light spots are staining artifacts, [37]); scale bar corresponds to 200 nm. (e) Schematic picture of the self-assembly and subsequent cross-linking of PB_{32}–PEO_{29}–X in methanol.

only one peak for the diblock copolymer. From ^{1}H NMR in $CDCl_3$ solution, the degree of functionalization of the PEO-sided carboxylate end group was determined to be larger than 85% for all samples. In addition, the numbers in the sample codes indicate the number average degree of polymerization of the individual blocks as determined by ^{1}H NMR.

3. Results and discussion

The self-assembly of poly(1,2-butadiene)-*b*-poly(ethylene oxide) diblock copolymers (PB–PEO) in water as selective solvent for PEO has been described by Jain et al. [14], which has led to a phase diagram of the morphologies built by these block copolymers in aqueous solution. Maskos et al. and Won et al. have reported on the formation of, e.g. vesicle- or cylinder-based nanoparticles, respectively, observed after subsequent cross-linking of the PB [25,31]. The first-mentioned system has the advantage that no addition of cross-linker is needed—which might influence the morphology—because cross-linking is achieved by γ-irradiation in solution.

This approach has now been employed to construct a phase diagram of the nanoparticle architectures obtained after intra-micellar cross-linking of the self-assembled micellar morphologies in selective solvents for PEO such as water and methanol.

The amphiphilic PB–PEO diblock copolymers were synthesized via anionic polymerization, as schematically shown in Fig. 1. The corresponding characterization is summarized in Table 1. The sample codes indicate the number average degree of polymerization of each block and in addition the PEO-sided end group introduced by the termination reaction.

3.1. Cross-linking via γ-irradiation in solution

As an example, the conversion of the cross-linking of $PB_{130}PEO_{120}$–H in methanol and water at a concentration of $c =$ 1.00 g/L as a function of the radiation dose is shown in Fig. 2.

The conversion was determined by the decrease in the RI signal intensity of the oligomer peak observed in GPC. In methanol, the dose necessary for complete conversion of the self-assembled diblock copolymers into the nanoparticles is determined via exponential growth fit to approximately 100 kGy, whereas in water 10 kGy are already sufficient. This corresponds to the observation that methanol is the less selective solvent and in addition can serve more easily as radical chain transfer agent. Nevertheless, inter-particle or

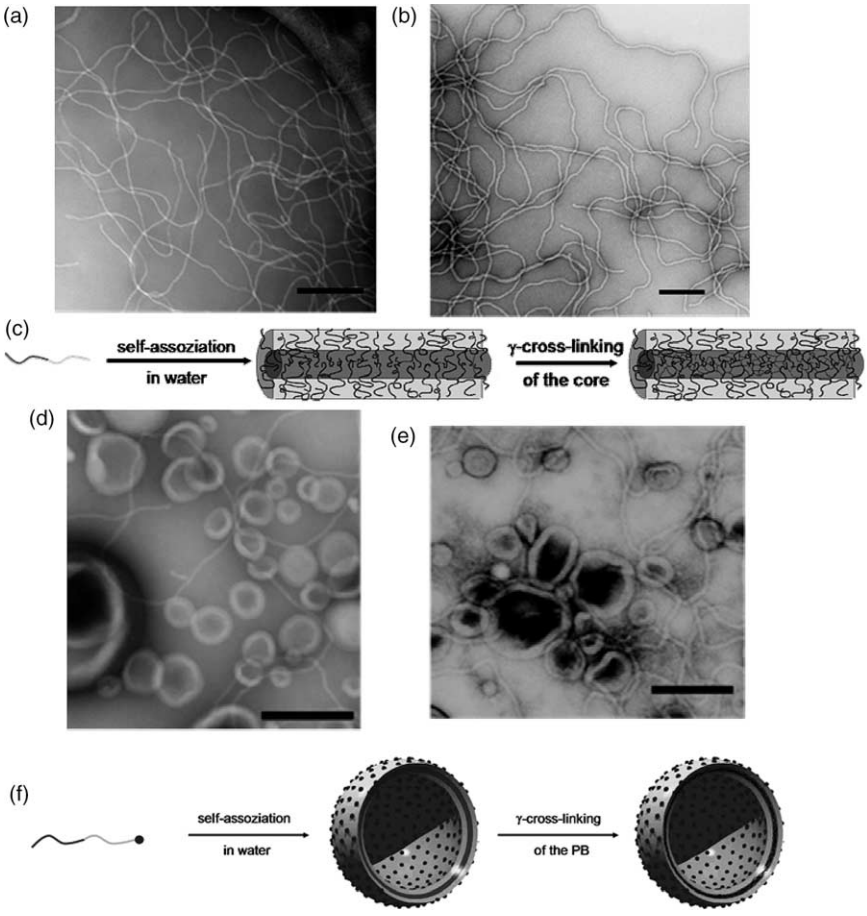

Fig. 4. TEM pictures of PB_{32}–PEO_{29}–H (a) and (b) and PB_{32}–PEO_{29}–COOK (d) and (e), after cross-linking in water ((a) and (d) $c = 1.1$ g/L) and after transfer of the fixed nanoparticles into THF ((b) and (e) $c = 0.2$ g/L); negatively stained with uranyl acetate ((a) and (d) 2 wt% aqueous solution, (b) and (e) saturated solution in DMF); scale bar corresponds to 250 nm; (c) and (f) corresponding schematic picture of the self-assembly and subsequent cross-linking of PB_{32}–PEO_{29}–X in water.

macroscopic cross-linking did not occur at these concentrations.

3.2. Influence of the solvent and the PEO-sided end group

As an example, the morphology of the cross-linked self-assemblies of the diblock copolymers $PB_{32}PEO_{29}$–H (Fig. 3(a)) and $PB_{32}PEO_{29}$–COOK (Fig. 3(c)) in methanol as observed in TEM are shown in Fig. 3.

Both diblock copolymers are identical, except of the PEO-sided end group and form spherical micelles leading to spherical nanoparticles with a cross-linked PB core and a PEO corona after γ-irradiation (Fig. 3(e)). In addition, the particles do not fall apart upon transfer into THF, which is a good solvent for both blocks, as also seen by TEM (Fig. 3(b) and (d), respectively).

If the self-assembly is performed in water, which is more selective for PEO as compared to methanol, the morphologies change (Fig. 4(a) and (d), respectively).

$PB_{32}PEO_{29}$–H forms cylindrical nanoparticles after cross-linking (Fig. 4(c)), whereas in case of $PB_{32}PEO_{29}$–COOK, mostly vesicle-based nanoparticles are obtained (Fig. 4(f)).

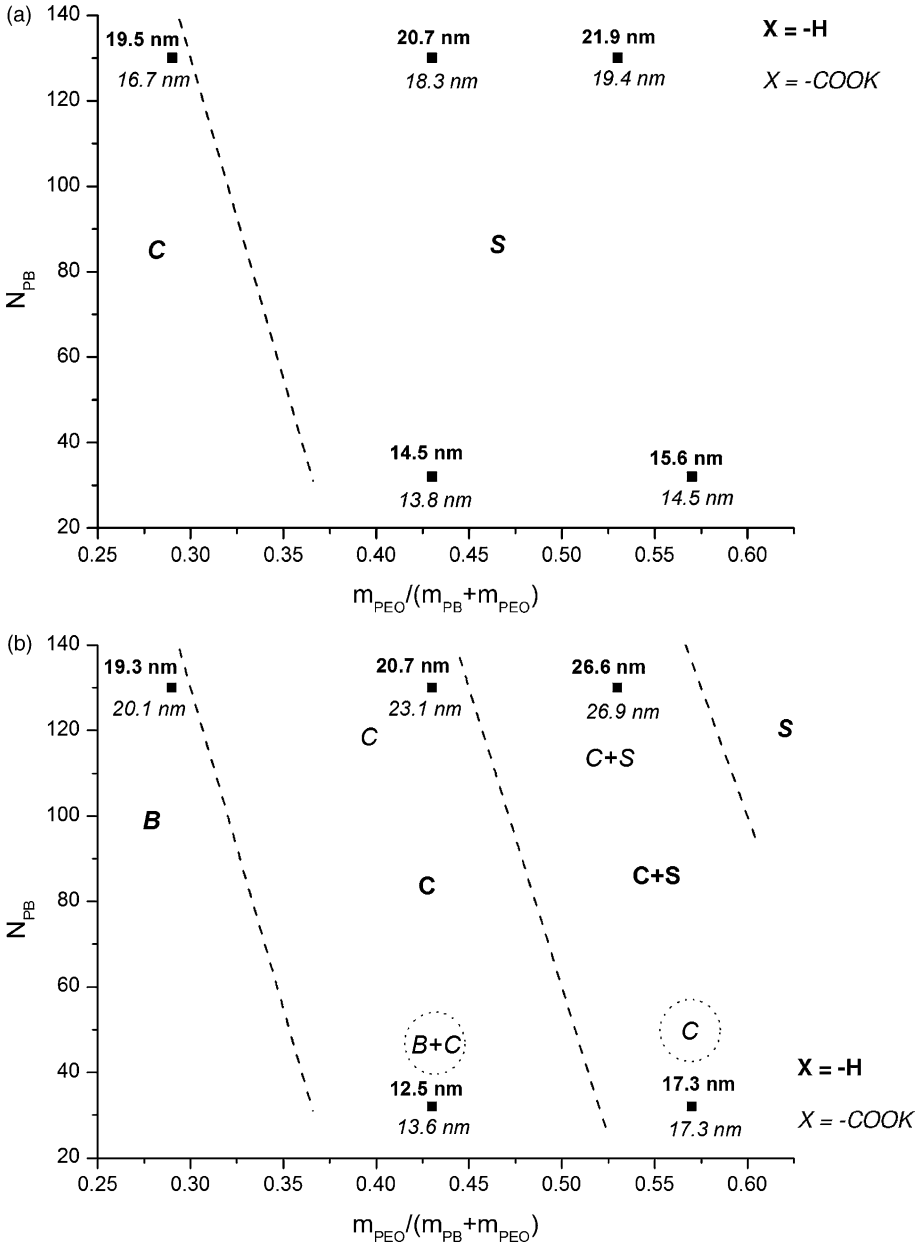

Fig. 5. Phase diagram of cross-linked PB_x–PEO_y–H and PB_x–PEO_y–COOK in methanol (a) and in water (b): number of PB repeating units (N_{PB}) as function of weight ration of PEO. The morphologies observed are indicated by S, spheres; C, cylinders; B, bilayers (vesicle-based); observed for PB_x–PEO_y–H: bold, observed for PB_x–PEO_y–COOK: italics, observed for both: bold and italics. The lines serve as guide for the eye and do not represent actual morphological borderlines. Characteristic dimensions D_c (diameter of a sphere, cross-section of a cylinder or bilayer, respectively) are provided for the individual nanoparticles in bold PB_x–PEO_y–H and in italics for PB_x–PEO_y–COOK. Highlighted by the dashed circles: major differences in morphology between PB_x–PEO_y–H and PB_x–PEO_y–COOK based nanoparticles.

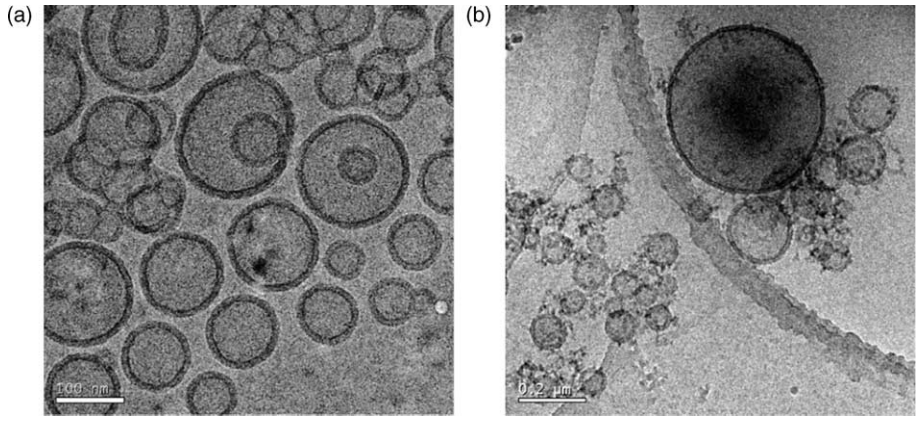

Fig. 6. Cryo-TEM pictures of PB_{130}–PEO_{66}–COOK before cross-linking ((a) scale bar 100 nm, $c = 1.0$ g/L) and after cross-linking in water ((b) scale bar 200 nm, $c = 1.0$ g/L).

This effect is attributed to the influence of the PEO-sided end group and is discussed together with the observations accompanied with the phase diagrams in the following section. Again, the successful locking-in of the morphology is demonstrated by the transfer into THF (Fig. 4(b) and (e), respectively).

3.3. Phase diagrams of the cross-linked nanoparticles

The morphologies of the diblock copolymers PB_xPEO_y–H in aqueous solution as obtained by cryo-TEM experiments (data not shown) match the observations for the non-cross-linked samples made by Jain et al. [14] and are presented in a phase diagram (Fig. 5(b)).

All synthesized nanoparticles were transferred into tetrahydrofurane (THF) without disintegration, which—as already discussed above—provides evidence for their structural integrity.

At concentrations up to approximately 5 g/L in water before cross-linking, it is observed by, e.g. dynamic light scattering or atomic force microscopy (data not shown) that the cross-linked nanoparticles are redispersible as single particles. At 10 g/L and above, which corresponds to the semi-concentrated regime, inter-connected structures possessing the same characteristic dimensions D_c are obtained after cross-linking, which e.g. for the cylindrical morphologies leads to the formation of macroscopic networks.

Fig. 5 also contains the characteristic dimensions D_c of the individual architectures of the nanoparticles obtained from the TEM measurements. For all samples discussed here, the characteristic dimensions, i.e. the micellar diameter for the spherical micelles, the diameter of the cylinders in case of the cylindrical micelles and the thickness of the lamella for the vesicles, correspond to structures with the hydrophobic PB as core and the hydrophilic PEO as corona. Except for the spherical micelles, the particle sizes, i.e. the length of the cylinders and the diameter of the vesicles, are influenced by the size polydispersity mainly introduced by the direct dissolution of the diblock copolymers in the selective solvent without addition of a co-solvent. This method for the sample preparation has been chosen because: (i) the glass transition temperature of the hydrophobic block PB is far below room temperature and, therefore; (ii) the complex removal of the co-solvent influencing the morphology can be avoided in the presented system [6].

The phase diagram of PB_xPEO_y–H in methanol (Fig. 5(a)) is shifted to higher curvature of the diblock copolymer surfactant according to Israelachvili [38], as expected due to the fact that methanol is the less selective solvent as compared to water. This also leads to smaller characteristic dimensions obtained for the nanoparticles in methanol as compared to water.

The phase diagrams discussed so far are related to diblock copolymers having a PEO-sided hydroxy end group. Subtle, but important differences are observed for diblock copolymers PB_xPEO_y–COOK containing a PEO-sided carboxy end group. The corresponding phase diagram of the nanoparticles after cross-linking in methanol is also presented in Fig. 5(a). The morphologies observed after cross-linking are identical to PB_xPEO_y–H, only the characteristic dimensions D_c are slightly smaller for PB_xPEO_y–COOK.

The phase diagram for cross-linked PB_xPEO_y–COOK in water is shown in Fig. 5(b). As an example, the cryo-TEM pictures obtained before and after cross-linking in water for $PB_{130}PEO_{66}$–COOK are presented in Fig. 6(a) and (b), respectively, and show identical characteristic dimensions.

The analysis of the Guinier-regime in the SANS scattering data of the sample before cross-linking in D_2O (Fig. 7) yields results for the characteristic dimension D_c, i.e. the lamellar thickness that are comparable to the data obtained from the cryo-TEM pictures.

Overall, the resulting morphology of the nanoparticles in water is ‘quasi-shifted’ towards a higher ratio of PB for the PB_xPEO_y–COOK as compared to PB_xPEO_y–H and the characteristic dimensions D_c are slightly larger for the carboxy-terminated diblock copolymers. Both observations indicate a slightly increased stretching of the PEO corona chains as compared to the hydroxyl-terminated block copolymers, which can be explained by a repulsion of the carboxylate end groups and the PEO at the experimental pH = 7. Similar interactions have been investigated and observed by Jiang et al.

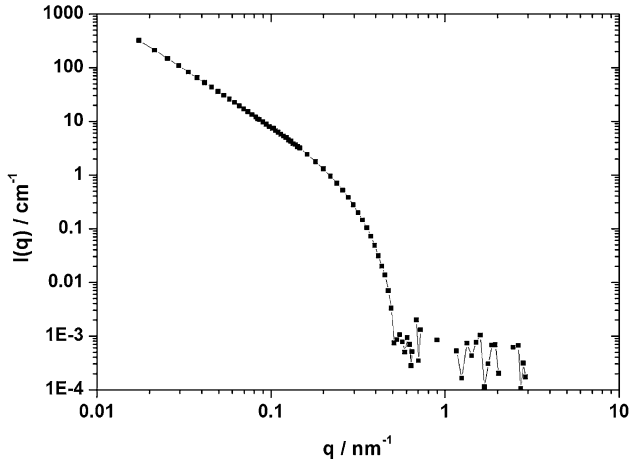

Fig. 7. SANS of PB_{130}–PEO_{66}–COOK in D_2O ($c=1.0$ g/L). Linear fit of the Guinier-regime ($q<0.1$ nm) yields radius of gyration of $R_g=5.8$ nm and bilayer thickness $D_c=20.1$ nm according to $D_c=12^{(1/2)}R_g$ [39].

for the pH-depending interaction of carboxylate groups and PEO by chemical force microscopy [40]. A very weak attraction was determined at pH = 2.5, whereas repulsion is found for pH ≥ 5.

In addition, no pronounced effect of the PEO-sided end group is observed in methanol in this part of the phase diagram, which could be explained by the more alike interaction properties of PEO and methanol as compared to water.

4. Conclusion

It has been shown that the morphologies observed by the self-assembly of PB–PEO diblock copolymers in selective solvents for PEO are successfully locked-in by the intramicellar cross-linking of the PB by γ-irradiation. The corresponding nanoparticles are transferred into the good solvent THF without structural disintegration of the amphiphilic nanoparticles. In addition, it is observed that a PEO-sided carboxy end group shifts the architecture of the resulting nanoparticles to a quasi-higher PB content as compared to a hydroxy end group. This effect is nearly negligible in the less selective solvent methanol. Nevertheless, an impact of the end group on the characteristic dimension of the nanoparticles is observed in water and in methanol.

Acknowledgements

M.M. would like to thank the Leopoldina, Deutsche Akademie der Naturforscher, for financial support, A. Eisenberg, McGill University, Montreal, Canada, for the great possibility to spend some time in his esteemed research lab, O. Rheingans and K. Fischer for the help in the synthesis of the diblock copolymers, and J.R. Harris for help in the TEM measurements, U. Kolb and M. Stepputat for the cryo-TEM measurements and F. Gröhn for the SANS measurements.

References

[1] Discher DE, Eisenberg A. Science 2002;297:967.
[2] Allen C, Han J, Yu Y, Maysinger D, Eisenberg A. J Control Release 2000; 63:275.
[3] Allen C, Eisenberg A, Mrsic J, Maysinger D. Drug Deliv 2000;7:139.
[4] Riegel IC, Samios D, Petzhold CL, Eisenberg A. Polymer 2003;44:2117.
[5] Choucair A, Lavigueur C, Eisenberg A. Langmuir 2004;20:3894.
[6] Cameron NS, Corbierre MK, Eisenberg A. Can J Chem 1999;77:1311.
[7] Hayashi H, Iijima M, Kataoka K, Nagasaki Y. Macromolecules 2004;37: 5389.
[8] Iijima M, Nagasaki Y, Okada T, Kataoka K. Macromolecules 1999;32: 1140.
[9] Antonietti M, Förster S. Adv Mater 2003;15:1323.
[10] Kukula H, Schlaad H, Antonietti M, Förster S. JACS 2002;124:1658.
[11] Meier W. Chem Soc Rev 2000;29:295.
[12] Nardin C, Bolikal D, Kohn J. Langmuir 2004;20:11721.
[13] Lombardo D, Micali N, Villari V, Kiselev MA. Phys Rev E 2004;70: 021402.
[14] Jain S, Bates FS. Macromolecules 2004;37:1511.
[15] Jain S, Bates FS. Science 2003;300:460.
[16] Photos PJ, Bacakova L, Discher B, Bates FS, Discher DE. J Control Release 2003;90:323.
[17] Won Y-Y, Brannan AK, Davis HT, Bates FS. J Phys Chem B 2002;106: 3354.
[18] Lee JC-M, Bermudez H, Discher BM, Sheehan MA, Won Y-Y, Bates FS, et al. Biotechnol Bioeng 2001;73:135.
[19] Napoli A, Valentini M, Tirelli N, Müller M, Hubbell JA. Nat Mater 2004; 3:183.
[20] Harris JK, Rose GD, Bruening ML. Langmuir 2002;18:5337.
[21] Qiu XP, Liu GJ. Polymer 2004;45:7203.
[22] Ding J, Liu G. J Phys Chem B 1998;102:6107.
[23] Henselwood F, Liu GJ. Macromolecules 1997;30:488.
[24] Guo A, Liu GJ, Tao J. Macromolecules 1996;29:2487.
[25] Maskos M, Harris JR. Macromol Rapid Commun 2001;22:271.
[26] Rheingans O, Hugenberg N, Harris JR, Fischer K, Maskos M. Macromolecules 2000;33:4780.
[27] Turner JL, Wooley KL. Nano Lett 2004;4:683.
[28] Kao HM, O'Connor RD, Mehta AK, Huang HY, Poliks B, Wooley KL, et al. Macromolecules 2001;34:544.
[29] Huang H, Kowalewski T, Remsen EE, Gertzmann R, Wooley KL. J Am Chem Soc 1997;119:11653.
[30] Discher BM, Bermudez H, Hammer DA, Discher DE, Won Y-Y, Bates FS. J Phys Chem B 2002;106:2848.
[31] Won Y-Y, Davis HT, Bates FS. Science 1999;283:960.
[32] Duz JZ, Chen YM, Zhang YH, Han CC, Fischer K, Schmidt M. JACS 2003;125:14710.
[33] Checot F, Lecommandoux S, Klok HA, Gnanou Y. Eur Phys J E 2003;10: 25.
[34] Gu CF, Chen DY, Jiang M. Macromolecules 2004;37:1666.
[35] Brown RA, Masters AJ, Price C, Yuan XF. In: Allen SG, Bevington JC, Booth C, Price C, editors. Comprehensive polymer science: polymer properties, vol. 2. Oxford: Pergamon; 1989.
[36] Bates FS, Fredrickson GH. Annu Rev Phys Chem 1990;41:525.
[37] Harris JR, Roos C, Djalali R, Rheingans O, Maskos M, Schmidt M. Micron 1999;30:289.
[38] Israelachvili JN. Intermolecular and surface forces. 2nd ed. London: Academic Press; 1992.
[39] Feigin LA, Svergun DL. In: Taylor GW, editor. Structure analysis by small angle X-ray and neutron scattering. New York: Plenum Press; 1987.
[40] Jiang X, Ortiz C, Hammond PT. Langmuir 2002;18:1131.